

## Strain state in silicon structures for microprocessor technology\*

M. HECKER\*\*, H. GEISLER

AMD Saxony LLC & Co. KG, Materials Analysis Department,  
Wilschdorfer Landstrasse 101, D-01109 Dresden, Germany

A promising approach to improve the performance of present CMOS devices is to introduce mechanical strain into the channel regions below the transistor gates. Strain can be generated as global strain on the whole wafer level (e.g., by growing strained silicon films on strain-relaxed silicon-germanium (SiGe) alloy layers or by using strained silicon films on an insulator), or as local strain on the transistor scale by applying specific technology processes (e.g., making use of embedded SiGe source-drain regions). The detection of strain in very thin silicon films requires sophisticated techniques with high depth sensitivity, whereas the measurement of the local strain state in thin Si structures with small lateral dimensions below 50 nm – such as the channels of current CMOS transistors – still remains to be mastered. A technique possessing the potential for solving this problem is Raman spectroscopy, where the diffraction limit for lateral resolution can be bypassed by near-field approaches. In the present paper, the occurrence of large strains in SiGe films and corresponding stresses in the GPa range are demonstrated by Raman spectroscopy, utilizing a simple approach for determining strain and composition separately. To estimate the strain distribution in a silicon channel structure due to embedded SiGe source-drain regions, a silicon strain calculation is applied based on a continuum-mechanical model utilizing a continuous distribution of virtual dislocations along the Si-SiGe boundaries. Within the framework of this model, the stress state in a 2D approximation is obtained by analytical expressions. Thus, the spatial distribution of channel strain and the impact of geometry on the strain state are obtained in a straightforward way.

Key words: *strain; silicon-germanium; Raman spectroscopy; stress modelling*

### 1. Introduction. Strained Si films for CMOS devices

Strained silicon thin films have not only been the focus of basic research during the last years, but nowadays are also used in the production process of microprocessor devices. On one hand, strain and corresponding stress in microelectronic systems are

---

\*Presented at the joint events 1st Workshop “Synthesis and Analysis of Nanomaterials and Nanostructures” and 3rd Czech-Silesian-Saxony Mechanics Colloquium, Wrocław, Poland, 21–22 November, 2005.

\*\*Corresponding author, e-mail: michael.hecker@amd.com

often a reliability issue, e.g. in interconnect lines and dielectric films where effort is made to avoid undesired stress. On the other hand, positive effects of strain are employed in CMOS transistor technology. The reason is a significant performance gain achievable by introducing strained films into active transistor regions [1, 2] which will become more important as the long-term scaling of device dimensions cannot be continued in the future without changing materials and technology. Issues connected with other performance enhancement steps, for example carrier mobility degradation observed due to new high- $k$  gate oxides, can be partially compensated by introducing strain, thus making it a key approach for extending CMOS to the next technology nodes [3].

The effect of strain on device performance is caused by an enhanced mobility of electrons or holes in the strained silicon regions which results from a modification of the silicon band structure. Strain can suspend the degeneracy of different valence bands, modify the band gap and band curvature, yielding a decrease of inter-valley scattering and a reduction of the effective charge carrier mass  $m^*$  [3]. Therefore, the mobility of the charge carriers  $\mu \sim 1/m^*$  increases, which in turn leads to a reduction in the resistance part of the transistor RC-delay and enables higher transistor frequencies.

Strain can be introduced into thin silicon film structures by several methods, e.g. employing different coefficients of thermal expansion for adjacent materials in combination with thermal treatments, or making use of lattice mismatch for epitaxially grown films. For the latter method, materials with similar crystallographic structure and deviating lattice parameters are needed, for example diamond being the material with the smaller lattice parameter and germanium the material with the larger lattice parameter (Table 1). Since the lattice misfit of these materials with respect to silicon is too large to obtain coherent growth of films with reasonable thickness, it is important that these materials show solubility in silicon and allow the fabrication of alloys with tuneable lattice constants. In particular, silicon–germanium alloys (SiGe) have been used to generate strain in Si films for improved CMOS performance [4].

Table 1. Lattice parameter  $a_0$ , mismatch strain  $\varepsilon_m$  (for a layer coherently on Si), elastic constants  $C_{ij}$  (Voigt's notation) for (001) oriented crystals, and corresponding charge carrier mobility for electrons ( $\mu_e$ ) and holes ( $\mu_h$ ) in silicon (Si), germanium (Ge), and diamond (C) [5, 6]

	Si	Ge	C
$a_0$ [nm]	0.3571	0.3567	0.3567
$\varepsilon_m = (a_{\text{Si}} - a_0)/a_0$	0	−4%	52%
$C_{11}$ [GPa]	165.7	128.4	1076.4
$C_{12}$ [GPa]	63.9	48.2	125.2
$C_{44}$ [GPa]	79.6	66.6	577.4
$\mu_e$ [cm <sup>2</sup> /Vs]	1500	3900	1800
$\mu_h$ [cm <sup>2</sup> /Vs]	450	1900	1600

In order to apply these materials to strain the silicon lattice, they must be either in a nearly strain-free state or strained in such a way that a certain lattice mismatch with

respect to bulk silicon is maintained at the interface between these materials and silicon. A customary method of achieving this is to deposit a composition-graded SiGe film on top of silicon, which contains lattice defects to compensate the strain mismatch, and to cap this film by an almost defect-free SiGe film with a lattice parameter corresponding to its constant chemical composition, i.e. in a strain relaxed state. A layer of silicon deposited on top of this stack will then become biaxially tensile strained according to the smaller lattice parameter of Si compared to the alloy (Fig. 1a). Since this technique provides a strained silicon film on the whole wafer level, it is known as the global strain technique.

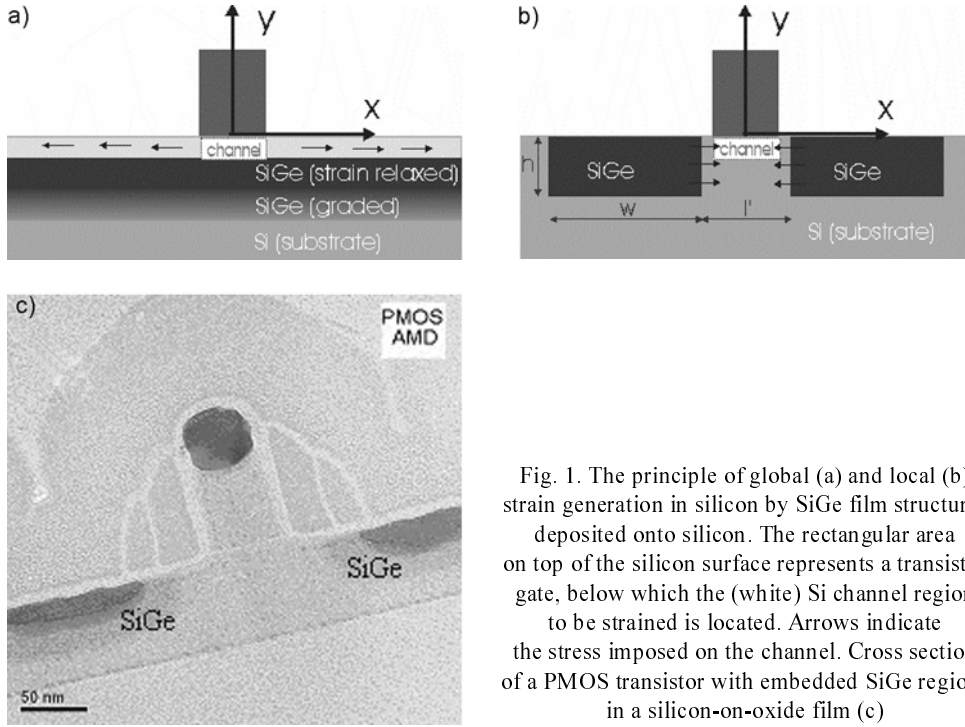


Fig. 1. The principle of global (a) and local (b) strain generation in silicon by SiGe film structures deposited onto silicon. The rectangular area on top of the silicon surface represents a transistor gate, below which the (white) Si channel region to be strained is located. Arrows indicate the stress imposed on the channel. Cross section of a PMOS transistor with embedded SiGe regions in a silicon-on-oxide film (c)

If a biaxial tensile strain of  $\sim 1$  GPa is reached in the top silicon film, the electron mobility can be improved by  $\sim 50\%$  [7], thus yielding an enormous performance gain for NMOS transistors. On the other hand, an increased mobility of holes determining the switching speed of PMOS transistors requires compressive strain which can be achieved by using  $\text{Si}_{1-x}\text{C}_x$  alloy layers instead of SiGe films. To tune the speed of both transistor types independently on a wafer, a local approach is needed (Fig. 1b). By depositing a SiGe alloy into etched Si cavities, a highly selective epitaxial SiGe growth with coherent interfaces to the surrounding silicon can be achieved, resulting in compressive strain within the SiGe region [3]. Depending on the geometry, this strain is also partially transferred to the surrounding silicon, yielding a compressive strain state in channel regions between the SiGe cavities and thus improving the per-

formance of the corresponding PMOS transistors. Usually, the strain state in the channel is denoted as uniaxial [3]. As will be shown in Section 3, the strain is non-uniform inside the channel, and the distribution between the strain components appearing to depend strongly on the given geometry. For advanced CMOS technologies, several methods to induce channel strain, such as embedded SiGe deposition, compressively and tensile stressed cap films (liners), and stress memorization techniques, are combined [8]. Moreover, combinations of global and local strain generation are expected to boost CMOS performance [9]. Thus, both the measurement and calculation of strain in such structures is required to achieve a better understanding of the strain state and its dedicated improvement of technological progress.

## 2. Strain measurement of SiGe films by Raman spectroscopy

To determine strain on non-patterned silicon film stacks, several methods, including high-resolution X-ray diffraction, wafer-curvature measurements by light deflection techniques, and Raman spectroscopy, can be applied. Among these, Raman spectroscopy has not only an excellent lateral resolution reaching the sub-micron scale, but has the potential to be scaled down to the nm-range by combining it with near-field optical techniques. The experimental challenges of making the so-called nano-Raman technique available for strained silicon analysis with high spatial resolution are discussed in [10]. With the common  $\sim 1 \mu\text{m}$  lateral resolution of confocal micro-Raman microscopes, Raman spectroscopy is already a precise strain measurement technique, with the additional advantage of high sample throughput due to short measurement time.

Nonetheless, simultaneous analysis of chemical composition and strain in thin films is difficult by Raman spectroscopy, since the Raman frequencies used for evaluation are sensitive to both, and the intensity from very thin films is weak. In principle, the different dependences of Raman peak positions on composition and strain in certain ranges of film thickness and composition can be utilized. In the following it will be shown that for epitaxial SiGe films in the range of the germanium content  $x$  between 10 at. % and 50 at. %, the separation of both effects can be achieved by determining the frequency of the Si–Si and Si–Ge phonon modes of the films, and that huge strains in the GPa range are accessible.

The instrument used was a Jobin Yvon Micro-Raman confocal microscope with a 488 nm wavelength Ar laser and ca.  $1 \mu\text{m}$  spot size. Figure 2 shows the results of measurements for two SiGe films epitaxially grown on (001) silicon. Apart from the silicon bulk signal emerging at the wavenumber  $\omega = 521 \text{ cm}^{-1}$ , characteristic peaks of the film appear corresponding to the excitations of Si–Si, Si–Ge, and Ge–Ge lattice phonons. In particular, the observation of the latter two modes is a challenge in the case of thin silicon-rich films.

In addition to the Si–Si phonon mode of the SiGe film, the Si–Ge mode was also evaluated, whereas the Ge–Ge phonon mode is very weak, especially for the low content range of Ge.

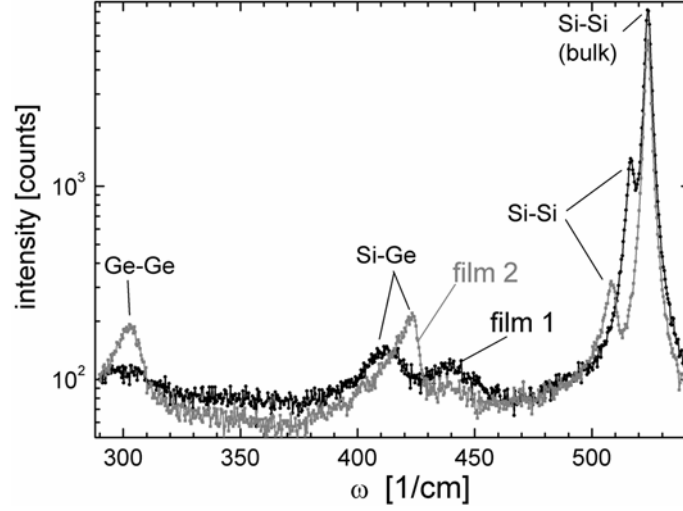


Fig. 2. Raman measurements of two  $\text{Si}_{1-x}\text{Ge}_x$  films grown coherently on (001)-Si. The parameters  $t$  for film thickness and  $x$  for Ge content as determined by high-resolution X-ray diffraction are  $t_1 = 57$  nm,  $x_1 = 22.2$  at. % and  $t_2 = 18$  nm,  $x_2 = 46.8$  at. % for film 1 and film 2, respectively

Figure 3 suggests a linear composition dependence for the peak position of the strained films (in a certain composition range). A linear dependence with a different slope was obtained for strain-relaxed SiGe alloys [11], suggesting a general dependence of the following type:

$$\Delta\omega = \omega - \omega_0 = \alpha x + \beta x \frac{\varepsilon_{\parallel}}{\varepsilon_{\parallel, \max}} \quad (1)$$

where  $\omega_0$  is the Raman wavenumber for the strain-free state with vanishing Ge content ( $x \rightarrow 0$ ),  $\alpha$  and  $\beta$  are constants,  $\varepsilon_{\parallel}$  is the in-plane strain of the SiGe film, and  $\varepsilon_{\parallel, \max}$  is the maximum in-plane SiGe strain achievable for the given composition  $x$  assuming fully coherent film growth, i.e.

$$\varepsilon_{\parallel, \max} = \frac{a_{\text{Si}} - a_{\text{SiGe}}}{a_{\text{SiGe}}} \quad (2a)$$

and  $a_{\text{SiGe}}$  is the strain-free alloy lattice parameter determined for the Dismuke's law [12]:

$$a_{\text{SiGe}} = a_{\text{Si}} + a'x + a''x^2 \quad (2b)$$

with  $a' = 0.01992$  nm and  $a'' = 0.002733$  nm. The ratio  $\varepsilon_{\parallel}/\varepsilon_{\parallel, \max}$  is a measure of the film strain degree and equals  $1 - R$ , with  $R$  being the usual relaxation degree of an epitaxial film. Considering a range of values for  $\alpha$  (e.g.,  $\alpha_{\text{Si-Si}}$  from  $-62$   $\text{cm}^{-1}$  to  $-70$   $\text{cm}^{-1}$ ) [11, 13]) for both the Si-Ge and Si-Si modes, from Fig. 3a, b it results that  $\beta_{\text{Si-Ge}} \sim \beta_{\text{Si-Si}} = \beta \sim 30$ . Within this approximation, the Ge content  $x$  and in-plane

strain  $\varepsilon_{||}$  can be derived from the measurement of the peak shifts  $\Delta\omega_{\text{Si-Si}}$  and  $\Delta\omega_{\text{Si-Ge}}$  using Eq. (1) for the Si-Si and Si-Ge modes, which yields:

$$x = \frac{\Delta\omega_{\text{Si-Si}} - \Delta\omega_{\text{Si-Ge}}}{\alpha_{\text{Si-Si}} - \alpha_{\text{Si-Ge}}} \quad (3a)$$

$$\varepsilon_{||} = \frac{\Delta\omega_{\text{Si-Si}} - x\alpha_{\text{Si-Si}}}{x\beta} \quad \varepsilon_{||, \max} = - \frac{\Delta\omega_{\text{Si-Si}} - x\alpha_{\text{Si-Si}}}{\beta} \frac{a' + a''x}{a_{\text{Si}} + a'x + a''x^2} \quad (3b)$$

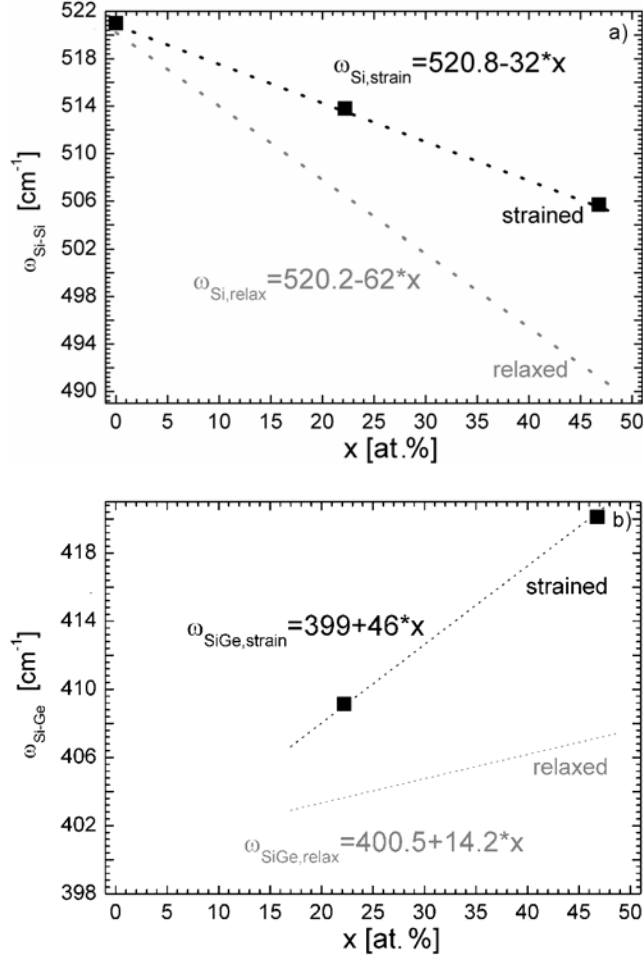


Fig. 3. Raman peak position of the Si-Si mode (a) and of the Si-Ge mode (b) for the measurements shown in Fig. 2, compared to data for bulk (strain relaxed) SiGe [11]

These relations provide an easy and straightforward way of determination of strain and composition in SiGe films with  $0.2 < x < 0.5$ . The observation of similar strain-

shift coefficients for both phonon modes is a rough approximation but it agrees with the measurements of Lockwood et al. [14]. Also, the dependence of the strain induced part of the Raman shift  $\Delta\omega_\epsilon$  and the in-plane strain  $\epsilon_{||}$ , written as  $\Delta\omega_s = b\epsilon_{||}$  [14] can be derived. For vanishing Ge content, from Eq. (1):

$$b(x=0) = -\frac{a_{\text{Si}}}{a'}\beta \quad (4)$$

with the value of  $b \sim -820 \text{ cm}^{-1}$  inferred, which is in the reported range  $-(715-832) \text{ cm}^{-1}$  (cf. [14]). Further measurements to improve the precision of these evaluations and to refine Eq. (3) are ongoing.

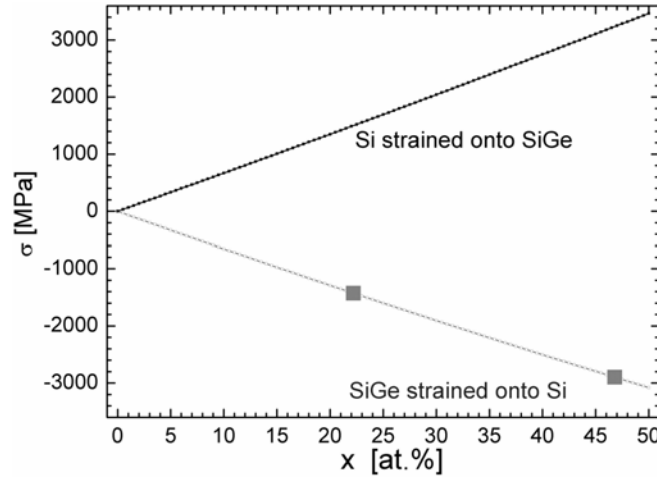


Fig. 4. Biaxial film stress of a  $\text{Si}_{1-x}\text{Ge}_x$  film deposited in a fully strained state onto Si (lower line) with the two data points corresponding to Fig. 2, and the film stress of a Si film fully strained on a  $\text{Si}_{1-x}\text{Ge}_x$  substrate (upper line)

The stress  $\sigma_{ij}$  in the SiGe films is obtained via Hooke's law:

$$\sigma_{ij} = C_{ijkl} \epsilon_{kl} \quad (5)$$

( $C_{ijkl}$  – elastic constants of the SiGe film,  $\epsilon_{kl}$  – elastic film strain components), assuming linear elasticity. For the presupposed biaxial strain state:

$$\epsilon_{11} = \epsilon_{22} = \epsilon_{||}, \quad \epsilon_{33} = \epsilon_{\perp}, \quad \epsilon_{ij} = 0 \ (i \neq j) \quad (6a)$$

with vanishing stress normal to the free surface

$$\sigma_{33} = 0 \quad (6b)$$

resulting from Eq. (5) for the biaxial stress  $\sigma = \sigma_{11} = \sigma_{22}$  in a (001)-oriented film

$$\sigma = \left( C_{11} + C_{12} - 2 \frac{C_{12}^2}{C_{11}} \varepsilon_{\parallel} \right) \quad (7)$$

where the elastic constants  $C_{ij}$  of the SiGe alloy can be approximated by the linear rule of mixtures from those of Si and Ge [15]

$$C_{ij} = xC_{ij,\text{Ge}} + (1-x)C_{ij,\text{Si}} \quad (8)$$

Figure 4 shows the degree of stress attainable in strained SiGe films, calculated according to Eq. (4) with values corresponding to the measurement results given in Figs. 2 and 3. If in turn a Si film can be grown coherently on top of a defect-free unstrained SiGe substrate, stresses of similar magnitude but opposite in sign arise in the silicon (Fig. 4, upper curve).

### 3. Model calculations for strained Si regions between SiGe cavities

The strain in a coherently grown film with a given lattice mismatch to the substrate, as represented in Fig. 1a, can be directly determined from Eq. (7) as a homogeneous number within the film, whereas a strain or stress distribution has to be considered for patterned structures as in local strain generation (Fig. 1b). A detailed estimation of the strain state requires many structural details to be considered and is usually achieved by numerical methods such as FEM simulations [7]. Some basic aspects of the impact of geometry on the local strain state can also be derived analytically. In the following, a simple two-dimensional approach is discussed, considering SiGe regions as coherent inclusions in the sense of Eshelby [16] with a stress-free strain  $\varepsilon^*$  according to the lattice mismatch to Si, embedded in an isotropic Si matrix. The strain determined by an inclusion approach can be alternatively formulated using the model of continuously distributed virtual surface dislocations, as utilized in [17, 18] for modelling cubic and prismatic precipitates. Figure 5 represents the principle of virtual edge dislocations distributed along SiGe cavity interfaces. The defects are described by the ratio  $s$  between the Burgers vectors  $b_e$  of the edge dislocations and their separation distance  $l_e$ , corresponding to the stress-free strain:

$$\varepsilon^* = \frac{a_{0,\text{SiGe}} - a_{\text{Si}}}{a_{0,\text{SiGe}}} = s = \frac{b_e}{l_e} \quad (9)$$

As pointed out in [16–18], the distribution of continuous dislocation can be considered to be equivalent to two-dimensional defects, conveniently described as Somigliana dislocations [19]. Figure 5a illustrates that each component  $\varepsilon_{11}^*$  and  $\varepsilon_{22}^*$  of the stress-free strain corresponds to two dipoles of Somigliana dislocations (SDs), introduced along the four interfaces of a rectangular SiGe region. Each SD thus corresponds to a semi-infinite distribution of edge dislocations (Fig. 6).



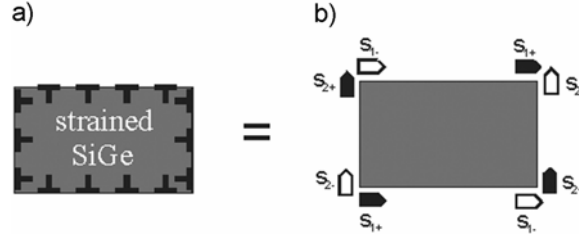


Fig. 5. Modelling of a strained SiGe region by a continuous distribution of virtual interface dislocations (a). Filled and empty symbols (b) represent SDs with positive and negative strengths  $s_+$  and  $s_-$  in an equivalent description by pairs of SD dipoles

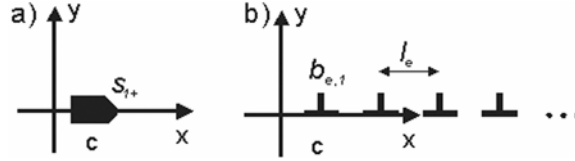


Fig. 6. SD  $s_{1+}$  (a) located at a distance  $c$  from the origin of the  $x$ -axis, according to a semi-infinite row of continuously distributed edge dislocations (b), with the defect strength parameter  $s_1 = b_{e,1}/l_e$ . A defect  $s_{1-}$  corresponds to a semi-infinite row of edge dislocations with the opposite Burgers vectors distributed along the  $x$ -axis, and SDs  $s_2$  are obtained by a distribution of edge dislocations parallel to the  $y$ -axis with the Burgers vector  $b_{e,2}$

The elastic fields for both orientations of the SDs within the  $xy$ -plane, described by indices 1 and 2 as the components of the Burgers vectors in the  $x$ - and  $y$ -directions, respectively, can be obtained by integrating the elastic fields of the equivalent edge dislocations [18], resulting in the following non-vanishing stress components for a defect  $s_{1+}$  (cf. Fig. 6a):

$$\sigma_{xx} = \frac{Gs_1}{2\pi(1-\nu)} \left\{ \frac{(x-c)y}{(x-c)^2 + y^2} - 2\arctan \frac{(x-c)}{y} - \pi \operatorname{sgn} y \right\} \quad (10a)$$

$$\sigma_{yy} = -\frac{Gs_1}{2\pi(1-\nu)} \frac{(x-c)y}{(x-c)^2 + y^2} \quad (10b)$$

$$\sigma_{xy} = \frac{Gs_1}{2\pi(1-\nu)} \left\{ \frac{1}{2} \ln[(x-c)^2 + y^2] + \frac{y^2}{(x-c)^2 + y^2} \right\} \quad (10c)$$

$$\sigma_{zz} = \nu(\sigma_{xx} + \sigma_{yy}) \quad (10d)$$

with the shear modulus  $G$  and Poisson's ratio  $\nu$ , related to  $C_{ij}$  for a (001)-orientation by:

$$G = C_{44}, \quad \nu = \frac{C_{12}}{C_{11} + C_{12}} \quad (11)$$

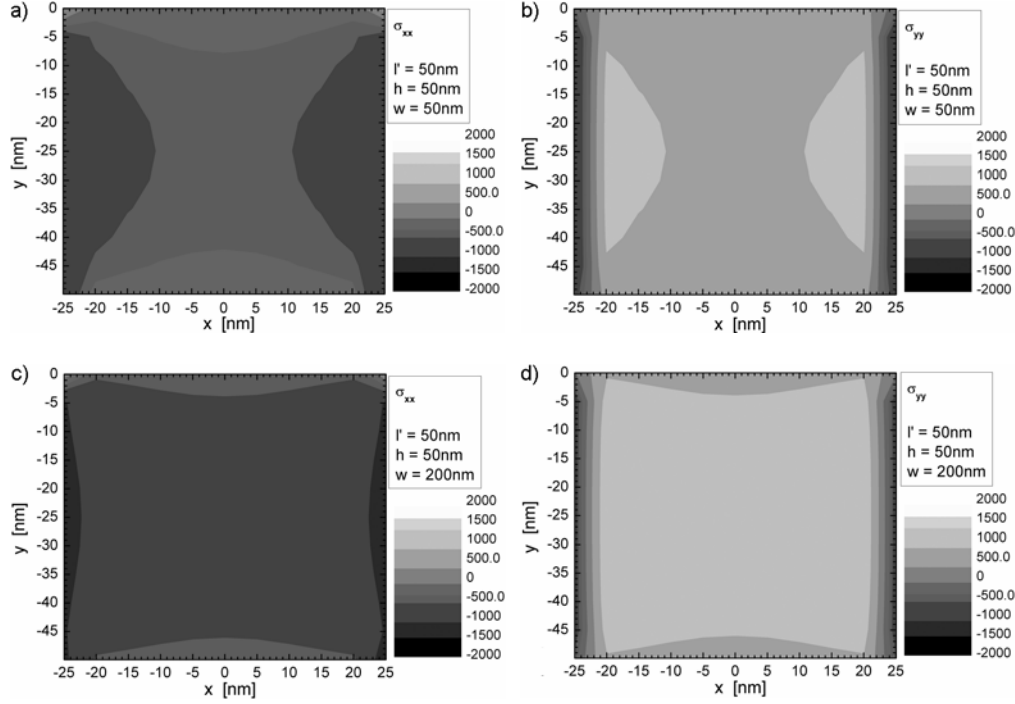


Fig. 7. Distributions of the stress components  $\sigma_{xx}$  (a, c) and  $\sigma_{yy}$  (b, d) in the channel region between two SiGe cavities with a square cross sections ( $w = h = 50$  nm, a, b) and rectangular cross sections ( $h = 50$  nm,  $w = 200$  nm, c, d). The scale is given in MPa. The assumed lattice misfit of 1% corresponds to  $x = 26.6$  at. % according to (2b). In a planar Si film fully strained on a SiGe substrate with this misfit, stresses of  $\sim 1800$  MPa would arise

The corresponding fields of SDs  $s_2$  can be obtained by coordinate transformation. Isoline maps of the 2D-stress fields obtained after summing up fields according to Figs. 1b and 5b are represented in Fig. 7. In these maps, two SiGe cavities are considered, with channel boundaries at  $x = \pm 25$  nm and in the  $y$ -range between 0 and  $-50$  nm. The gate structure, the lower elastic constants of SiGe ( $\sim 94\%$  of the Si constants for the given concentration), and the surface on top are neglected in this approach. In particular, the upper surface should modify the stress distribution within the channel. Nevertheless, some general tendencies for the impact of geometry on the stress state can be derived already from this simple approach. The stress state within the channel is thus not really uniaxial and restricted to the component  $\sigma_{xx}$ , but a perpendicular stress component of opposite sign occurs. Both local distribution and mean stress within the channel region depend on the cavity geometry. Figures 7c, d show, in comparison to Figs. 7a, b, that an elongation of the SiGe regions in the  $x$ -direction with unchanged channel structure yields a significant increase in the magnitude of both channel stress components. This tendency is also reflected in Fig. 8 for the central line  $x = 0$  between the SiGe regions, showing a stress reduction of  $\sim 200$  MPa for a change from the elongated cavity cross section to a square-like one. Furthermore, Figure 8 shows how an

increase of the stress component  $\sigma_{xx}$  can be achieved by reducing the distance  $l'$  between the cavities or by increasing their height  $h$  (cf. Fig. 1b).

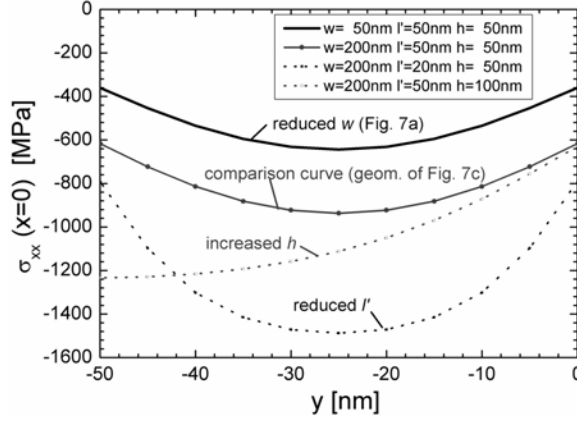


Fig. 8. Distribution of the stress  $\sigma_{xx}$  along a line in the channel centre ( $x = 0$  nm) between SiGe regions with different geometric parameters for a lattice misfit of 1%

These results show that the geometry of SiGe cavities has an important impact on the stress component  $\sigma_{xx}$  which is directly related to the charge carrier mobility in the  $x$ -direction according to the piezoelectric tensor of Si [20]. For a detailed discussion of the distribution of all stress components, a subsequent refinement of the present approach is necessary, taking into account different elastic properties in the SiGe cavities and in the surface on top of the cavities. The approach can be based on stress fields of virtual dislocations at interfaces of isotropic media [21], considering the impact of a surface on the SD stress fields [22].

#### 4. Conclusions

In summary, the problem of local stress in silicon structures used for CMOS technology was approached both experimentally and by modelling. It was shown that Raman spectroscopy is an appropriate technique to derive SiGe film stress and composition. For that purpose, a simple relationship between the Raman shifts of two phonon modes, composition, and stress was derived. High stress levels in strained SiGe films were obtained. Though the Raman measurements were performed with a spatial resolution of only  $\sim 1\mu\text{m}$ , highly improved lateral resolution can be obtained by combining a near-field Raman approach with AFM techniques. The need for higher strain resolution is motivated by the requirement to understand stress state on the device scale in present and future CMOS technologies. A link between strain measurements and technology development can be provided by modelling on the device scale, which requires close feedback to measurements. To estimate the local stress state in patterned silicon structures, an analytic approach for calculating the local distribution is

introduced, which can yield general tendencies important for understanding the mechanisms and for further improving the performance of devices. According to calculation results, effective methods for increasing the magnitude of the (compressive) channel stress  $\sigma_{xx}$  should be elongating the SiGe cavities in the  $x$ -direction and reducing their distance  $l'$ . Within the framework of the used analytic approach, the implementation of different elastic moduli of Si and SiGe, of surface effects, and of the 3D shape of strained regions, as considered in [17, 21, 22], is possible.

#### Acknowledgements

Valuable discussions with Ehrenfried Zschech, AMD Saxony, Dresden (Germany), are gratefully acknowledged. For TEM we are grateful to Hans-Jürgen Engelmann, also with AMD Saxony, Dresden (Germany).

#### References

- [1] WELSER J., HOYT J.L., TAGAKI S., GIBBONS, F.J., IEDM Tech. Dig., 1994, 373.
- [2] HOYT J.L., NAYFEH H.M., EGUCHI S., ABERG I., XIA G., DRAKE T., FITZGERALD E.A., ANTONIADIS D.A., IEDM Tech. Dig., 2002, 23.
- [3] MOHTA N., THOMPSON S.E., IEEE Circuits Dev. Mag., 9/10 (2005), 18.
- [4] LEE M.L., FITZGERALD E.A., BULSARA M.T., CURRIE M.T. LOCHTEFELD A., J. Appl. Phys., 97 (2005), 011101.
- [5] EBERL K., SCHMIDT O.G., DUSCHL R., [in:] *Properties of Silicon Germanium and SiGe: Carbon*, E. Kasper, K. Lyutovich (Eds.), INSPEC London (2000), p. 75.
- [6] ANASTASSAKIS E., SIAKAVELLAS M., J. Appl. Phys., 90 (2001), 144.
- [7] MOROZ V., XU X., PRAMANIK D., NOURI F., KRIVOKAPIC Z., Sol. State Techn., 7 (2004), 49.
- [8] HORSTMANN M., WEI A., KAMMLER T., HÖNTSCHL J. BIERSTEDT H., FEUDEL T., FROHBERG K., IEDM Tech. Dig. (2005), 243.
- [9] IRISAWA T., NUMATA T., TEZUKA T., USADA K., NAKAHARAI S., HIRASHITA N., SUGIYAMA N., TOYODA E., TAGAKI S., IEDM Tech. Dig. (2005), 727.
- [10] ZHU L., ATEANG J., DUDEK P., HECKER M., RINDERKNECHT J., RITZ Y., GEISLER H., HERR U., GEER R., ZSCHECH E., Mater. Sci.-Poland, 27 (2007), 19.
- [11] TSANG J.C., MOONEY P.M., DACOL F., CHU J.O., J. Appl. Phys., 75 (1994), 8098.
- [12] DISMUKES J.P., EKSTROM L., PAFF R.J., J. Phys. Chem., 68 (1964), 3021.
- [13] ALONSO M.I., WINER K., Phys. Rev. B, 39 (1989), 10056.
- [14] LOCKWOOD D.J., BARIBEAU J.M., Phys. Rev. B, 45 (1992), 8565.
- [15] FLORO J.A., CHASON E., LEE S.R., PETERSEN G.A., Appl. Phys. Lett., 71 (1997), 1694.
- [16] ESHELBY J.D., Proc. Royal Soc., A241 (1957), 376.
- [17] KROUPA F., LEJCEK L., Czech. J. Phys., B20 (1970), 1063.
- [18] BONNET R., MARCON G., ATI A., Phil. Mag (A), 51 (1985), 429.
- [19] SOMIGLIANA, C., Atti. Accad. Naz. Lincei Rc., 23 (1914) 463.
- [20] SMITH C.S., Phys. Rev. B, 94 (1954), 42.
- [21] NAKAHARA S., WU J.B.C., LI J.C.M., Mat. Sci. Engn., 10 (1972), 291.
- [22] ROMANOV A.E., HECKER M., phys. stat. sol. (a), 115 (1989), K159.

*Received 3 January 2006*

*Revised 28 May 2006*